Regularized pseudopotential for mean-field calculations

Regularized pseudopotential for mean-field calculations

K Bennaceur[1], J Dobaczewski[2,3,4], T Haverinen[3,5] and M Kortelainen[3,5]

[1] Univ Lyon, Université Claude Bernard Lyon 1, CNRS, IPNL, UMR 5822, 4 rue E. Fermi, F-69622 Villeurbanne Cedex, France
[2] Department of Physics, University of York, Heslington, York YO10 5DD, United Kingdom
[3] Helsinki Institute of Physics, P.O. Box 64, 00014 University of Helsinki, Finland
[4] Institute of Theoretical Physics, Faculty of Physics, University of Warsaw, Pasteura 5, 02-093 Warszawa, Poland
[5] Department of Physics, University of Jyväskylä, P.O. Box 35 (YFL), 40014 University of Jyväskylä, Finland

E-mail: `bennaceur@ipnl.in2p3.fr`

Abstract. We present preliminary results obtained with a finite-range two-body pseudopotential complemented with zero-range spin-orbit and density-dependent terms. After discussing the penalty function used to adjust parameters, we discuss predictions for binding energies of spherical nuclei calculated at the mean-field level, and we compare them with those obtained using the standard Gogny D1S finite-range effective interaction.

1. Introduction

A new class of pseudopotentials for nuclear structure were introduced several years ago [1, 2, 3]. These pseudopotentials allow for a consistent formulation of the low-energy energy-density-functional (EDF) approach in terms of effective theory. Specifically, this can be done by considering a zero-range effective interaction with derivative terms up to a given order $p = 2n$, hereafter denoted N^{n}LO [4], and replacing the contact Dirac delta function by a regulator,

$$g_a(\mathbf{r}) = \frac{\mathrm{e}^{-\frac{\mathbf{r}^2}{a^2}}}{\left(a\sqrt{\pi}\right)^3}, \tag{1}$$

where a is the range of the obtained pseudopotential or regularization scale.

In this work we complemented the regularized pseudopotential with the standard zero-range spin-orbit term and two-body zero-range density-dependent effective interaction. Therefore, the obtained EDF is meant to be used at the mean-field (single-reference) level. The density-dependent term represents a convenient way to adjust the nucleon effective mass in infinite nuclear matter to any reasonable value in the interval $0.70 \lesssim m^*/m \lesssim 0.90$ [5]. For this zero-range density dependent term, we use the same form as in the Gogny D1S interaction [6], *i.e.*,

$$\frac{1}{6}\, t_3 \left(1 + x_3\, \hat{P}_\sigma\right) \rho_0^{1/3}(\mathbf{r}_1)\delta(\mathbf{r}_1 - \mathbf{r}_2), \tag{2}$$

where $\hat{P}_\sigma$ is the spin-exchange operator and x_3 is fixed to 1, so for time-even invariant states, this term does not contribute to pairing. Finally, because of the zero-range nature of the spin-orbit term, we omitted its contribution to the pairing channel.

The general EDF derived from this pseudopotential [3], including its particle-hole and particle-particle parts, were limited to the local part. This could constitute a significant restriction to its flexibility. However, such a limitation reduces the number of free parameters to be adjusted and simplifies implementations in the existing codes.

After presenting the ingredients of the penalty function used to adjust the parameters, we present results obtained for binding energy of spherical nuclei along with their comparison with those obtained for the Gogny D1S functional.

2. Adjustments of parameters

The pseudopotentials considered here contain 10 parameters at NLO, 14 at N^{2}LO and 18 at N^{3}LO. We adjusted 15 series of parameters with effective masses of 0.70, 0.75, 0.80, 0.85, and 0.90 at NLO, N^{2}LO, and N^{3}LO. For each series, the range a of the regulator was varied from 0.8 fm to 1.6 fm.

The use of a penalty function containing data for finite nuclei would not be sufficient to efficiently constrain these parameters or even to constrain them at all. Typical reasons for this difficulty are: appearance of finite-size instabilities, phase transitions to unphysical states (for example, those characterized by a very large vector pairing) or numerical problems related to compensations of large coupling constants with opposite signs. To avoid these unwanted situations, the penalty function must contain specially designed constrains that we list here, along with the nuclear data and pseudo-data:

(i) Empirical quantities in infinite nuclear matter: saturation density $\rho_{\rm sat}$, binding energy per nucleon in symmetric matter E/A, compression modulus K_∞, isoscalar effective mass m^*/m symmetry energy coefficient J, and its slope L, see Table 1.

(ii) Decomposition of the potential energy in the different (S,T) channel [7, 8] and binding energy per nucleon in neutron and polarized matter.

(iii) Average pairing gap in infinite nuclear matter for $k_F = 0.4$, 0.8 and 1.2 fm^{-1} with the values obtained with D1S as targets.

(iv) Binding energies of the following 17 spherical (or approximated as spherical) nuclei ^{36}Ca, ^{40}Ca, ^{48}Ca, ^{54}Ca, ^{54}Ni, ^{56}Ni, ^{72}Ni, ^{80}Zr, ^{90}Zr, ^{112}Zr, ^{100}Sn, ^{132}Sn, ^{138}Sn, ^{178}Pb, ^{208}Pb, ^{214}Pb, and ^{216}Th with a tolerance of 1 MeV if the binding energy is known from experiment and 2 MeV if it is extrapolated (values are taken from [9]).

(v) Proton density rms radii (taken from [10]) for ^{40}Ca, ^{48}Ca and ^{208}Pb with a tolerance of 0.02 fm and 0.03 fm for the one of ^{56}Ni (extrapolated from systematics);

(vi) Isovector density at the center of ^{208}Pb and isoscalar density at the center of ^{40}Ca to avoid finite-size scalar-isovector (*i.e.* $S = 0, T = 1$) instabilities. The use of the linear response (as in Ref. [11] for zero-range interactions) would lead to too much time-consuming calculations. Therefore we use these two empirical constraints on these densities which are observed to grow when a scalar-isovector instability tends to develop. Possible instabilities in the vector channels ($S = 1$) are not under control in this series of fits.

(vii) Coupling constants for the vector pairing (given by eq. (36) in [3]) are constrained to be equal to 0 ± 5 MeV fm^3 to avoid transitions to unphysical states with unrealistically large vector pairing.

These adjustments were performed in three steps:

(i) First, we made exploratory adjustments (with fixed values for the effective mass) trying to determine whether the other canonical values for infinite nuclear matter were attainable and,

Table 1. Infinite nuclear matter targeted properties and tolerances used for the final step of the parameters adjustment.

Quantity	E/A [MeV]	$\rho_{\rm sat}$ [fm]$^{-3}$	K_∞ [MeV]	m^*/m	J [MeV]	L [MeV]
Value	-16.0	0.158	230	0.70-0.90	29.0	15.00
Tolerance	0.3	0.003	5	0.001	0.5	0.05

in this case, what would be their optimal values in average. We obtained $\rho_{\rm sat} = 0.158$ fm^{-3}, for the saturation density, $J = 29$ MeV for the symmetry energy coefficient and $L = 15$ MeV for its slope. This value for L is very low compared with what is considered as realistic nowadays [12, 13, 14] but we observed that larger values inevitably lead to finite-size instabilities.

(ii) With effective mass and $\rho_{\rm sat}$, J, and L fixed to these values, and for each value of the effective mass and order of the interaction, we systematically determined the ranges a of the regulator that give the lowest values of the penalty function.

(iii) With these values for the ranges fixed, we readjusted the parameters by relaxing values of $\rho_{\rm sat}$, m^*/m, J, and L and allowing for them narrow tolerances of $\rho_{\rm sat} = 0.158 \pm 0.003$ fm^{-3}, $m^*/m = 0.700 \pm 0.001$, $J = 29.0 \pm 0.5$ MeV, and $L = 15.00 \pm 0.05$ MeV.

The summary of targeted values and tolerances for infinite nuclear matter properties are given in Table 1. The targeted values and tolerances for all other data and pseudo-data will be given and motivated with more details in a forthcoming article [15].

3. Results and discussion

Questions concerning the dependence of the penalty function and observables on the range of the regulator, covariance analysis of the parameters and propagation of statistical errors on calculated quantities will not be discussed in this contribution where we only report results for spherical nuclei. The sets of parameters obtained by minimizing the penalty function will be given in [15].

We have built a set of 214 nuclei with even numbers of protons and neutrons which, according to the predictions obtained with the Gogny D1S interaction [16], can be considered as spherical or almost spherical. In Table 2, we report the obtained average root mean squared deviations $\sqrt{\overline{\Delta E^2}}$ and average deviations $\overline{\Delta E}$. We use the subscript "all" when these quantities are calculated for the full set of 214 even-even nuclei and the subscript "fit" when they are calculated for the 17 nuclei used in the penalty function only.

Since binding energies of nuclei are not the only ingredients used in the penalty function, there is no reason for $\sqrt{\overline{\Delta E^2}}_{\rm fit}$ to decrease when more parameters are used, *i.e.* to decrease with n for interactions at N^{n}LO. Nonetheless, we observe that it decreases with n for all constrained values of the effective mass. Interestingly, $\sqrt{\overline{\Delta E^2}}_{\rm all}$ is also a decreasing function of n for all values of the effective mass but for 0.7. This means that for $m^*/m \geqslant 0.75$, the increase of the number of parameters in the pseudopotential improves its predictive power, at least for the binding energies of spherical nuclei. The average deviation $\overline{\Delta E}_{\rm fit}$ is also a decreasing function of n while, in general, $\overline{\Delta E}_{\rm all}$ has a less regular behaviour, although it does decrease with n for $m^*/m = 0.85$.

To visualize the global behaviour of the results obtained for the binding energies of spherical nuclei, in Fig. 1 we plotted the binding energy residuals obtained for the set of 214 spherical

Table 2. Average root mean squared deviation ($\sqrt{\Delta E^2}$) and average deviation ($\overline{\Delta E}$) for 214 even-even nuclei (with subscript "all") and for the 17 nuclei used in the penalty function (with subscript "fit") for the pseudopotentials at NLO, N^{2}LO and N^{3}LO with effective mass from 0.70 to 0.90.

m^*/m		0.70	0.75	0.80	0.85	0.90
NLO	$\sqrt{\overline{\Delta E^2}}_{\rm all}$	1.840	1.759	1.801	1.929	2.141
	$\overline{\Delta E}_{\rm all}$	0.382	0.029	-0.301	-0.633	-0.950
	$\sqrt{\overline{\Delta E^2}}_{\rm fit}$	1.899	1.899	1.956	2.052	2.201
	$\overline{\Delta E}_{\rm fit}$	0.112	0.112	0.115	0.121	0.129
N^{2}LO	$\sqrt{\overline{\Delta E^2}}_{\rm all}$	2.028	1.827	1.709	1.594	1.540
	$\overline{\Delta E}_{\rm all}$	0.879	0.670	0.484	0.295	0.116
	$\sqrt{\overline{\Delta E^2}}_{\rm fit}$	1.893	1.741	1.690	1.610	1.602
	$\overline{\Delta E}_{\rm fit}$	0.111	0.102	0.099	0.095	0.094
N^{3}LO	$\sqrt{\overline{\Delta E^2}}_{\rm all}$	1.712	1.577	1.531	1.458	1.490
	$\overline{\Delta E}_{\rm all}$	0.378	0.231	-0.048	-0.105	-0.313
	$\sqrt{\overline{\Delta E^2}}_{\rm fit}$	1.587	1.446	1.690	1.264	1.228
	$\overline{\Delta E}_{\rm fit}$	0.093	0.085	0.080	0.074	0.072

Figure 1. Binding energy residuals obtained with the pseudopotentials with m^*/m constrained to 0.70 at order $n = 1$, 2 and 3 (black dots) compared with the ones obtained with the D1S Gogny interaction (open square).

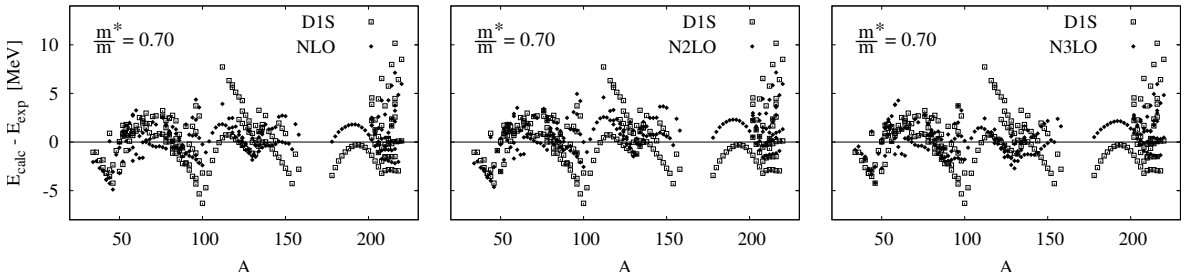

nuclei and for the pseudopotential with $m^*/m = 0.70$ at $n = 1$, 2, 3. Similarly, in Fig. 2, we plotted those obtained for the pseudopotentials with $m^*/m = 0.85$. We chose these two values because, on the one hand, $m^*/m = 0.70$ is close to the value obtained with D1S and, on the other hand, $m^*/m = 0.85$ is the effective mass that leads to the lowest value for $\sqrt{\overline{\Delta E^2}}_{\rm all}$ (obtained at N^{3}LO). In the same figures, to show the comparison with a commonly used finite-range interaction, we also plotted the residuals obtained for the Gogny D1S EDF. The comparison should be considered with caution, because the Gogny D1S interaction, although often used at the mean-field level only, is supposed to be used in beyond mean-field approaches, such as the 5-dimensional Collective Hamiltonian (known as 5DCH [17]) to provide observables that can be compared with experimental data.

Both figures show that the residuals obtained for the regularized pseudopotentials are more

Figure 2. Same as figure 1 for the pseudopotentials with m^*/m constrained to 0.85.

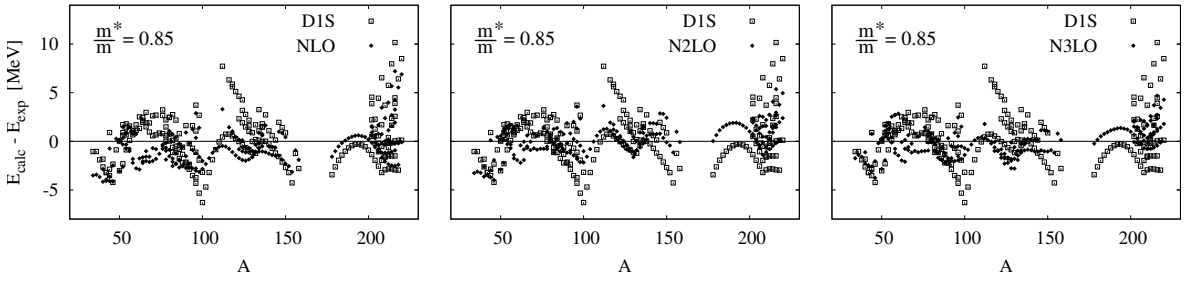

compressed around zero than those obtained for D1S. Fig. 1 explicitly exhibits the information already summarized in Table 2, *i.e.*, for the effective mass of 0.70, adding new parameters in the pseudopotential does not significantly improve the predictive power for the binding energies of spherical nuclei.

Comparing the results shown in Figs. 1 and 2, one can see that the typical arches appearing in the residuals between shell closures are significantly damped. Furthermore, one can see that this damping is more pronounced for higher order pseudopotentials.

4. Conclusion

In this article, we have reported results for binding energies of spherical nuclei obtained for the new class of pseudopotentials introduced several years ago [1, 2, 3]. A more complete study including the discussion of proton radii, single particle energies, and properties of deformed nuclei is in preparation. Although a definitive conclusion can only be drawn after a comparison of a larger body of observables with data, the studied class of pseudopotential looks promising. Possible improvements could still be the inclusion of non-local terms and the use of regularized spin-orbit and tensor terms [2, 3], which will be the subject of future developments. Which part of correlations can be incorporated into the coupling constants of the pseudopotential used at the mean-field (single-reference) level remains an open question.

Acknowledgments

This work was partially supported by the Academy of Finland under the Academy project no. 318043, by the STFC Grants No. ST/M006433/1 and No. ST/P003885/1, and by the Polish National Science Centre under Contract No. 2018/31/B/ST2/02220. We acknowledge the CSC-IT Center for Science Ltd. (Finland) and the IN2P3 Computing Center (CNRS, Lyon-Villeurbanne, France) for the allocation of computational resources.

References

[1] Dobaczewski J, Bennaceur K and Raimondi F 2012 *Journal of Physics G: Nuclear and Particle Physics* **39** 125103
[2] Raimondi F, Bennaceur K and Dobaczewski J 2014 *Journal of Physics G: Nuclear and Particle Physics* **41** 055112
[3] Bennaceur K, Idini A, Dobaczewski J, Dobaczewski P, Kortelainen M and Raimondi F 2017 *Journal of Physics G: Nuclear and Particle Physics* **44** 045106
[4] Carlsson B G, Dobaczewski J and Kortelainen M 2008 *Phys. Rev. C* **78**(4) 044326
[5] Davesne D, Navarro J, Meyer J, Bennaceur K and Pastore A 2018 *Phys. Rev. C* **97**(4) 044304
[6] Berger J, Girod M and Gogny D 1991 *Computer Physics Communications* **63** 365 – 374
[7] Baldo M, Bombaci I and Burgio G F 1997 *Astron. Astrophys.* **328** 274–282
[8] Baldo M 2016 private communication

[9] Wang M, Audi G, Kondev F G, Huang W, Naimi S and Xu X 2017 *Chinese Physics C* **41** 030003
[10] Kortelainen M, Lesinski T, Moré J, Nazarewicz W, Sarich J, Schunck N, Stoitsov M V and Wild S 2010 *Phys. Rev. C* **82**(2) 024313
[11] Hellemans V, Pastore A, Duguet T, Bennaceur K, Davesne D, Meyer J, Bender M and Heenen P H 2013 *Phys. Rev. C* **88**(6) 064323
[12] Li X H, Cai B J, Chen L W, Chen R, Li B A and Xu C 2013 *Physics Letters B* **721** 101 – 106 ISSN 0370-2693
[13] Lattimer J M and Lim Y 2013 *The Astrophysical Journal* **771** 51
[14] Roca-Maza X, Viñas X, Centelles M, Agrawal B K, Colò G, Paar N, Piekarewicz J and Vretenar D 2015 *Phys. Rev. C* **92**(6) 064304
[15] Bennaceur K, Dobaczewski J, Haverinen T, Kortelainen M and Pastore A in preparation
[16] Hilaire S and Girod M 2008 *AIP Conference Proceedings* **1012** 359–361
[17] Libert J, Girod M and Delaroche J P 1999 *Phys. Rev. C* **60**(5) 054301